Engineering Structures 130 (2017) 83–98

Contents lists available at ScienceDirect

Engineering Structures

journal homepage: www.elsevier.com/locate/engstruct

Simplified reliability analysis of punching in reinforced concrete flat slab buildings under accidental actions

P. Olmati [a,1], J. Sagaseta [b,*], D. Cormie [c], A.E.K. Jones [c]

[a] University of Surrey, UK[2]
[b] Department of Civil and Environmental Engineering, University of Surrey, Guildford GU2 7XH, UK
[c] Arup, London W1T 4BQ, UK

ARTICLE INFO

Article history:
Received 13 January 2016
Revised 10 June 2016
Accepted 27 September 2016
Available online 17 October 2016

Keywords:
Punching
Flat slabs
Reliability analysis
Progressive collapse
Dynamic amplification factor
Finite element analysis
Column failure
Floor impact
Explosion load

ABSTRACT

Flat slab concrete buildings are widely found in infrastructure such as office and residential buildings or industrial facilities. The susceptibility of progressive collapse of such structures due to accidental loads is highly dependent on the structural performance of the slab-column connections. This paper presents a framework for a simplified reliability analysis and derivation of safety factors for computing the probability of punching of flat slab concrete buildings subjected to accidental loads such as column removal, slab falling from above or blast load. The main advantage of the proposed approach is that it considers in a simple manner, the uncertainty in the gravity load applied in the slab before the accidental event, which affects the inertial effects and demand/capacity ratio in the slab-column connections. Eurocode 2 and the Critical Shear Crack Theory for punching are used and extended to dynamic cases for the assessment of the demand/capacity ratio using computer-based time history finite element simulations. The proposed reliability method is applied to a case study of an existing building showing that the column removal situation is not always critical whereas the slab falling from above is much more detrimental.

1. Introduction

1.1. Progressive collapse of flat slab buildings

Concrete flat slab structures is a common form of structural reinforced concrete (RC) construction in buildings, especially in medium-rise offices due to their efficient span/depth ratios and the economies gained by reducing the storey heights. A governing aspect in the design of RC flat slabs is the detailing of the slab-column connections in order to provide sufficient deformation and punching shear capacity of the slab at the connection. Structural failures of flat slab buildings due to punching have been reported in the past in America, Asia and Europe; some examples are the Skyline Plaza Complex collapse in Virginia (1973), the Harbour Cay building in Florida (1981), the Sampoong Department Store collapse in South Korea (1995) and the Gretzenbach underground parking garage collapse in Switzerland (2004). The reasons behind these failures include deficiencies in design, errors during execution and unforeseen actions; some of the causes mentioned are not unique to flat slab construction.

The main concern with flat slabs is that unless special measures are adopted, the shear capacity at the column-slab connection is low after punching failure which can contribute to a horizontal propagation of failure and subsequently the slab can fall onto the next lower floor [1]. Moreover, the propagation of failure (horizontally and vertically) is influenced by dynamic effects which can significantly increase the shear demand in the slab-column connections. As pointed out by Vlassis et al. [2], modelling the connection behaviour accurately is critical towards providing alternative load paths and achieving continuity and ductility in the structure.

1.2. Design considerations

Commercial and residential buildings are generally not designed to withstand extreme loads since the occurrence of such extreme events does not concern the life-cycle of the building due to the low probability of occurrence. However, exceptional loads due to extreme events could lead to severe consequences in terms of structural integrity and socio-economic impact on the community [3]. The term "disproportionate collapse" is often used to refer

* Corresponding author at: Faculty of Engineering and Physical Sciences, Civil Engineering C5, Guildford, Surrey GU2 7XH, UK.
E-mail address: j.sagaseta@surrey.ac.uk (J. Sagaseta).
[1] Current address: Tokyo Polytechnic University, Kanagawa, Japan.
[2] Formerly postdoc.

http://dx.doi.org/10.1016/j.engstruct.2016.09.061
0141-0296/

to the disproportion between the scale of the event and the severity of the consequences, although this term is subjective and it has several definitions [4]. Extreme events can be caused by natural hazards (hurricanes, tsunamis, flooding, earthquakes), accidents (vehicle impact, event during construction, industrial accident and unexpected local failure due to fire or poor design) and malicious actions (terrorist attack).

The perception from the general public and stakeholders of the risk of having disproportional collapse of buildings has increased significantly over the last two decades [5] and therefore robustness (insensitivity of the structure to local failure) must be verified in practice according to most designing codes (e.g. CEN [6]; DoD [7]; GSA [8]); guidelines are also available for example Ellingwood et al. [9], FEMA [10] or HSE [11]. In order to design against progressive collapse, prescriptive rules (indirect approaches) have been available since soon after the Ronan Point failure in 1968. Direct approaches are becoming more easily accessible to designers although the behaviour of buildings subjected to exceptional loads is still an under-researched area in structural engineering [12]. The alternate load path method as described in DoD [7] is widely used in practice to design buildings to withstand accidental loads. However, the applicability of this approach depends on the form of construction used affecting the behaviour of the connections, alternative load path mechanisms and energy dissipation of the system.

1.3. Literature review and research significance

Different progressive collapse analyses have been suggested in the past for steel frame buildings covering column removal and falling debris cases (e.g. Vlassis et al. [2]; Szyniszewski and Krauthammer [13]). Similarly, research on RC structures has been carried out predominately looking at beam-column frame structures [14,15] under column removal and impact scenarios. Beam-column-slab concrete buildings were also investigated numerically and experimentally by Helmy et al. [16] showing that the slab needs to be considered in the analysis to obtain accurate results.

Research on progressive collapse of flat slab buildings (without beams) is rather limited (e.g. Mitchell and Cook [17]; Utagawa et al. [18]; Qian and Bing [19]; Liu et al. [20,21]). Flat slabs provide enhanced structural continuity compared to frame structures. Moreover, the slabs are effective in providing alternative load paths due to the two-way bending and membrane actions [17,22–24]. However, flat slabs are prone to punching which is a brittle type of failure that should be controlled to arrest the progressive collapse of the structure. Relevant studies of the residual shear strength of the connection after failure (post-punching behaviour) were carried out by Melo and Regan [25] and Fernández Ruiz et al. [26] amongst others. The residual strength of the slab-column connection can vary between 25% and 50% [1] and the results are influenced by many factors such as anchorage or the presence of integrity reinforcement in the compressive zone.

The progressive collapse of flat slab buildings is highly influenced by the inertial effects of the slab. This paper presents a simple reliability approach for flat slab buildings which takes into account the inertial effects and considers the uncertainty in the gravity load applied in the slab and the dynamic response of the slab-column connection. The proposed approach requires computer-based dynamic structural analyses (time history analysis for punching) to estimate the variation of punching demand and capacity at the connections. The punching capacity is estimated based on EN 1992 [27] and the Critical Shear Crack Theory (CSCT) by Muttoni [28] and Fernández Ruiz and Muttoni [29], with special considerations for dynamic loading (see Section 2). Three extreme events are investigated in a case study, viz. column removal, falling slab from above and blast load. The proposed approach focuses on the prediction of failure of the connections during extreme events. The analysis of the propagation of the collapse is outside the scope of this paper; in such cases, system-based analyses are generally required considering the mechanisms that develop before and after punching (e.g. [20,21,24]).

2. Punching shear time history analysis

In this work, time history analyses are carried out for the assessment of punching shear in flat slab buildings subjected to different damage scenarios. In these analyses, the punching shear demand around the column is calculated numerically by means of finite element (FE) models (non-linear dynamic). Both punching shear demand and capacity are estimated at different time steps using design formulae for punching in EN 1992 [27] and the CSCT [28] which is the basis of the Model Code 2010 formulae for punching [30]. The main difference between the two approaches in dynamic situations is that the former assumes that the capacity is constant with time whereas the latter assumes that the capacity is a function of the slab rotation outside the column region $\psi(t)$ which varies with time. In both approaches, the punching shear demand $V_D(t)$ varies with time due to variations in the axial forces and moments developed in the columns and slab during the forced and free vibration phases.

2.1. Dynamic punching shear demand

Local damage in flat slab buildings can result in an increase in the moment transfer in the column-slab connections (increase in eccentricity of the reaction at the column). An increase in moment transfer will result in a higher concentration of shear forces in certain segments of the control perimeter adopted in the punching shear calculations which in turn results in a higher shear demand. This is taken into account in EN 1992 [27] by means of the eccentricity coefficient $\beta(t)$ given by Eqs. (1) and (2) for internal and edge/corner columns respectively.

$$\beta(t) = 1 + 1.8\sqrt{\left(\frac{e_y(t)}{b_x}\right)^2 + \left(\frac{e_x(t)}{b_y}\right)^2} \tag{1}$$

$$\beta(t) = \frac{u}{u_{red}} + k_a \frac{u}{W_1} e_{par}(t) \tag{2}$$

where u is the basic control perimeter defined in EN 1992 [27] at a distance $2d$ from the column face, $e_x(t)$ and $e_y(t)$ are the eccentricities in the two orthogonal directions of the slab, b_x and b_y are the dimensions of the control perimeter corresponding to each direction. Eq. (2) is for edge columns and it is reduced to its first term in case of corner columns; u_{red} is the reduced control perimeter according to geometric conditions given in [27], k_a and W_1 are coefficients which depend on the dimensions of the column and of the effective depth of the slab, and $e_{par}(t)$ is the eccentricity with respect to the bending of the slab along the edge. The punching shear stress demand $v_D(t)$ according to EN 1992 [27] is given by Eq. (3).

$$v_D(t) = \beta(t)\frac{V_D(t)}{ud} \tag{3}$$

In the CSCT, the eccentricity effect is taken into account similarly using a reduction factor $k_e(t)$ given by Eq. (4) which multiples the basic control perimeter b_0 to calculate the punching shear stress in Eq. (5). The basic control perimeter b_0 in the CSCT is taken at a distance equal to $0.5d$ from the column face.

$$k_e(t) = \frac{1}{1 + e_u(t)/b_u} \tag{4}$$

$$v_D(t) = \frac{V_D(t)}{k_e(t) b_0 d} \quad (5)$$

where b_u is the diameter of the circle with the same surface as the support region inside the basic control perimeter and $e_u(t)$ is the load eccentricity with respect to the centroid of the basic control perimeter. In Eqs. (1)–(5), the eccentricities are obtained from the bending moments at the columns given by the FE analysis just above and below the slab-column connection in both orthogonal directions; the punching shear demand around the column is obtained as the difference between the axial force in the column above and below the slab.

2.2. Dynamic punching shear capacity

2.2.1. EN 1992 formulae for punching capacity

The punching shear capacity $V_{C,cs}(t)$ is calculated at each time step by adding the concrete contribution $V_{C,c}(t)$ and the steel contribution from the shear reinforcement $V_{C,s}(t)$. Eqs. (6) and (7) from EN 1992 [27] were derived empirically from quasi-static loading slab tests and therefore they are time independent.

$$V_{C,c} = C_{C,c} k \sqrt[3]{100 \rho f_c} \cdot (ud) \quad (6)$$

$$V_{C,cs} = 0.75 V_{C,c} + V_{C,s} = 0.75 V_{C,c} + 1.5 \left(\frac{d}{S_r}\right) A_{sw} f_{yw,eff} \quad (7)$$

in SI units, where $C_{C,c} = 0.18$, $k = 1 + \sqrt{200/d} \leqslant 2$ with d in mm, S_r is the radial spacing between perimeters of shear reinforcement, A_{sw} is the area of one perimeter of shear reinforcement around the column, and $f_{yw,eff}$ is the effective strength of the punching shear reinforcement which is calculated as $f_{yw,ef} = 250 + 0.25d \leqslant f_{yw}$. Partial factors γ_c and γ_s were taken as 1. In Eq. (6), an additional term could be added according to EN 1992 which is a function of the normal stresses σ_{cp} (in-plane stress); favourable term (enhanced capacity) if in compression. This term could be used to consider potential capacity enhancement due to compressive membrane action. However, up to date there is no accurate method available to estimate σ_{cp} and in absence of a better approach, σ_{cp} is taken as zero in subsequent analysis. The effect of high strain-rates on material strength is also neglected in EN 1992 formulae.

2.2.2. Critical Shear Crack Theory (CSCT)

The main assumption in the CSCT is that the capacity is related to the crack width and roughness of the critical shear crack. The crack width is proportional to the slab rotation outside the column region which varies over time $\psi(t)$. The concrete $V_{C,c}(t)$ and steel contributions $V_{C,s}(t)$ are expressed as a function of the slab rotation and therefore they vary over time. The method is given by the following expressions

$$\frac{V_{C,c}(t)}{k_e(t) b_0 d \sqrt{f_c}} = \frac{0.75}{1 + 15\psi(t) \frac{d}{(d_{g0} + d_g)}} \quad (8)$$

$$V_{C,s}(t) = \sum A_{sw} \cdot k_e(t) \sigma_{sw}(t) \quad (9)$$

$$\sigma_{sw}(t) = \frac{E_s \psi(t)}{6} \left(1 + \frac{3}{f_{yw}} \frac{d}{\Phi_w}\right) \leqslant f_{yw} \quad (10)$$

$$V_{C,cs}(t) = V_{C,c}(t) + V_{C,s}(t) \quad (11)$$

where the shear and slab rotation $\psi(t)$ are normally expressed as normalized values: normalized shear $\overline{V} = V/(k_e b_0 d \sqrt{f_c})$ (in $\sqrt{\text{MPa}}$) and the normalized slab rotation $\bar{\psi} = \psi d/(d_g + d_{g0})$. Parameter d_g refers to the maximum aggregate size where $d_{g0} = 16$ mm is the reference size. Parameter $\sum A_{sw}$ is the total area of shear reinforcement within a conical surface with angle 45° from the support (zone limited by $0.35 d_v$ and d_v from the face of the column). σ_{sw} is the effective stress of the shear reinforcement (limited to the yield stress) which depends on the bond strength as shown in Eq. (10) which is written in terms of the Young's modulus E_s, bar diameter Φ_w and yield strength f_{yw}.

The slab rotation outside the column region $\psi(t)$ is estimated from a flexural analysis. In this work, $\psi(t)$ is estimated using FE analysis due to the complexity of the problems investigated (i.e. irregular geometry and dynamic conditions). Analytical formulae exist for $\psi(t)$ for simple cases such as quasi-static loading with unrestraint internal/edge/corner columns [28]. In this work, the slab rotation obtained from FE models correspond to the direction of the maximum rotations (e.g. span of removed column). More refined approaches are available for non-symmetric cases considering the slab rotations along both orthogonal directions [31], however considering the maximum rotation is more suitable for design purposes.

Eqs. (8)–(11) can be applied to dynamic situations as demonstrated by Micallef et al. [32] for impact loading. In such cases, high strain-rates $\dot{\varepsilon}$ can result in a slight increase in punching shear capacity; unless a more sophisticated analysis is carried out, it is demonstrated that coefficient 0.75 in Eq. (8) can be replaced by 0.8 for $\dot{\varepsilon} = 10/\text{s}$, 1.0 for $\dot{\varepsilon} = 100/\text{s}$ and 1.3 for $\dot{\varepsilon} = 300/\text{s}$ with linearly interpolated values for intermediate cases. Numerical predictions of strain rates in this work suggest that the strain-rate, governing the velocity of the opening of the shear crack, were well below 10/s; $\dot{\varepsilon}$ was around 0.02/s for the column removal, 0.04/s for falling slab scenario and 0.06/s for blast load case. This suggests that the quasi-static capacity in Eq. (8) can be adopted in subsequent analysis; furthermore this assumption is conservative and consistent with [7] recommendations for column removal analysis.

2.3. Calculation of performance function and demand ratio at each time step

The performance function [33] or limit state equation $Z(t)$ is introduced to assess at each time step whether punching shear occurs (i.e. $Z(t) < 0$). The demand and capacity are expressed as shear stresses in Eq. (12) using EN 1992 formulae whereas the normalized shear is used in the CSCT as shown in Eq. (13)

$$Z(t) = v_{C,cs} - v_D(t) \quad (12)$$

$$\overline{Z}(t) = \overline{V}_{C,cs}(t) - \overline{V}_D(t) \quad (13)$$

In order to compare both approaches with each other, the demand ratio $DR(t)$ is introduced which is the coefficient between the demand and capacity as shown in Eqs. (14) and (15).

$$DR_{EN\ 1992}(t) = \frac{v_D(t)}{v_{C,cs}} \quad (14)$$

$$DR_{CSCT}(t) = \frac{\overline{V}_D(t)}{\overline{V}_{C,cs}(t)} \quad (15)$$

Fig. 1 summarizes the flowcharts for the assessment of punching shear at each time step using EN 1992 and CSCT approaches. The structural analyses in this work neglect any post-failure effects in connections (post-punching behaviour) and therefore the algorithm shown in Fig. 1 is only valid for times t when DR is lower or equal to 1. For times after $DR > 1$, the stiffness of the slab-column connection would have to be re-assessed after failure to update the structural analysis. Such type of analysis would only be needed if the propagation of failure through the structure is to be assessed (e.g. [20,21,24]), which is not the main focus of this work. This work is primarily concerned with the probability of fail-

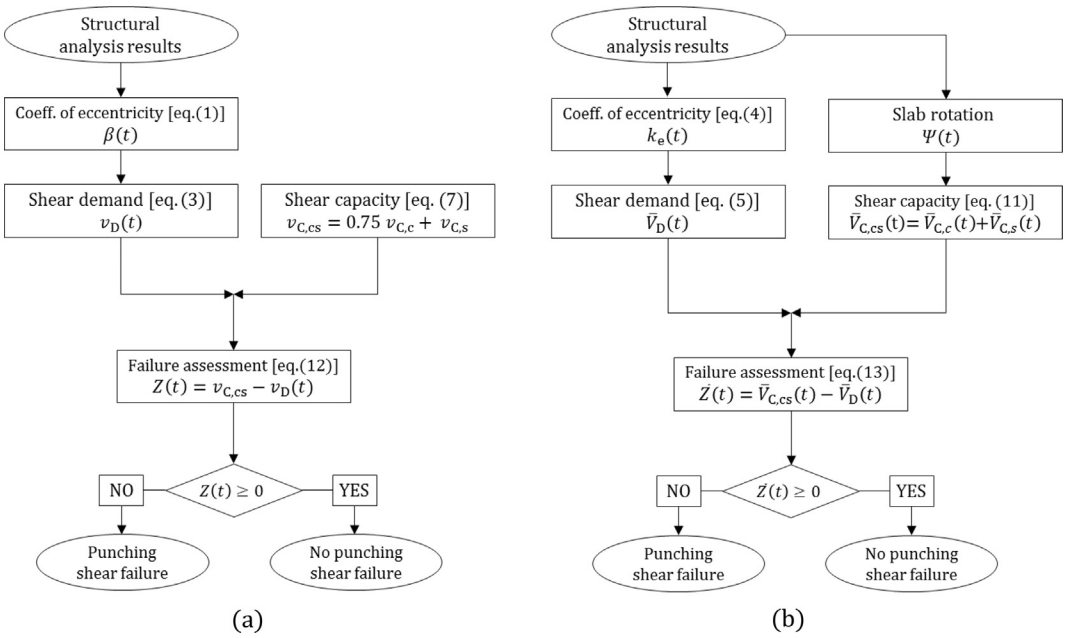

Fig. 1. Assessment of performance function at each time interval from structural analysis results using (a) EN 1992 [27] formulae for punching and (b) CSCT approach.

ure of an adjacent connection after column removal as described in the following section; other types of local damage are also investigated.

3. Case study: column removal in flat slab building

The column removal scenario, as described in [7], is the most common threat considered in the assessment of structural robustness of buildings since these structural elements have a key role in the progressive collapse [34]. The column removal is an idealised structural damage used to assess the ability of the building to provide alternative load paths without suffering a disproportionate collapse with respect to the initial structural damage. The column is instantaneously removed from the structure, without considering any surrounding damages which could occur due to the load causing the damage to the column. Therefore, this analysis looks at the indirect response of the building with focus on the consequences of the direct damage. The alternative approach would be to look at the direct response of the building, which would require to include also the load causing the damage (e.g. explosion, impact); this approach is normally restricted to single structural elements although it can also be applied to assess the global response of the building (e.g. far-field large explosions). This section is primarily concerned with the former approach (indirect response approach) applied to an existing office building described in Section 3.1. Section 5 focuses on direct approaches showing that particular cases such impact or blast are not necessarily covered by idealised column removal scenarios.

3.1. Description of the structure: geometry, materials, reinforcement and loading

The office building shown in Fig. 2 was selected by the authors for the column removal study. This structure described in CS [35] was designed using EN 1992. The structure consists of a 300 mm thick flat slab with an irregular column layout with spans ranging from 4 m to 9.6 m and 400 mm square columns (3.5 m storey height). This building corresponds to a real project in which the geometry, reinforcement layout, materials and design considerations are well documented [35]. Fig. 2(a) shows the plan view of the area of the building under consideration in which internal column C2 is removed in the analysis and the punching shear of connections B2 (internal column) and C3 (edge column) is assessed.

The material strengths are taken as the average values with no material partial safety factors applied in the analysis. The concrete in the slab is C30/37; the characteristic cylinder strength of 30 MPa is factored by 1.1 (average strength factor) and 1.1 (concrete aging factor) leading to an average compressive strength of 36.3 MPa. Equally the concrete in the columns is C50/60 with an average compressive strength of 60.5 MPa. The reinforcement steel is B500B with a characteristic strength of 500 MPa with an average strength factor of 1.1; average strength of 550 MPa. The flexural reinforcement layout is presented in Fig. 3 with top reinforcement ratios at the internal columns of 0.96% and 1.27% in the x and y directions respectively. Punching shear reinforcement is provided around internal and edge columns: 11 link legs of 10 mm diameter bars per perimeter (A_{sw} = 863 mm^2) with 175 mm radial spacing between shear reinforcement perimeters and 125 mm distance from the face of the column to the first reinforcement perimeter (3 perimeters of shear reinforcement are required for the internal columns whereas only two perimeters are needed for the edge columns). The flexural and punching shear reinforcement is taken directly from [35]; the reinforcement was designed according to EN 1992.

The specified imposed loading or live load (LL) in the design was 4 kN/m^2 and 1 kN/m^2 dead load (DL) which are values commonly adopted in design; for the roof only a nominal imposed load of 1 kN/m^2 was adopted in all the analyses unless specified otherwise. Four load combinations are considered in the column removal analyses which are summarized in Table 1. The combinations included quasi-permanent (DL + 0.3LL), frequent (DL + 0.5LL), characteristic (DL + LL) and overload (DL + 1.5LL) scenarios with an uniformly distributed load. The combination factors adopted for the quasi-permanent and frequent cases are consistent with EN 1990 [6] combination of actions for accidental loads in buildings with load categories A and B.

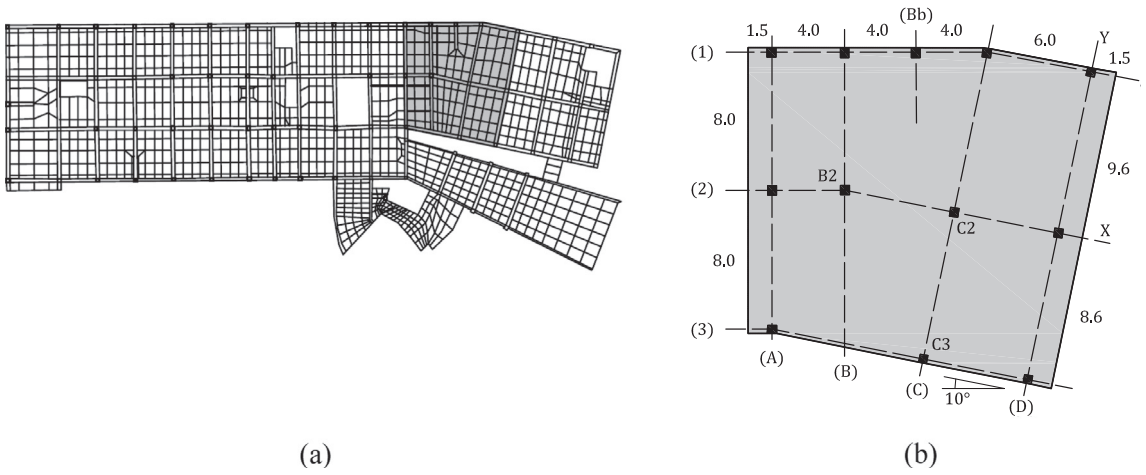

Fig. 2. Flat slab concrete building case study, adapted from CS [35]: (a) plan view of the office building (shaded area corresponds to area of study), (b) span layout of the modelled part of the structure.

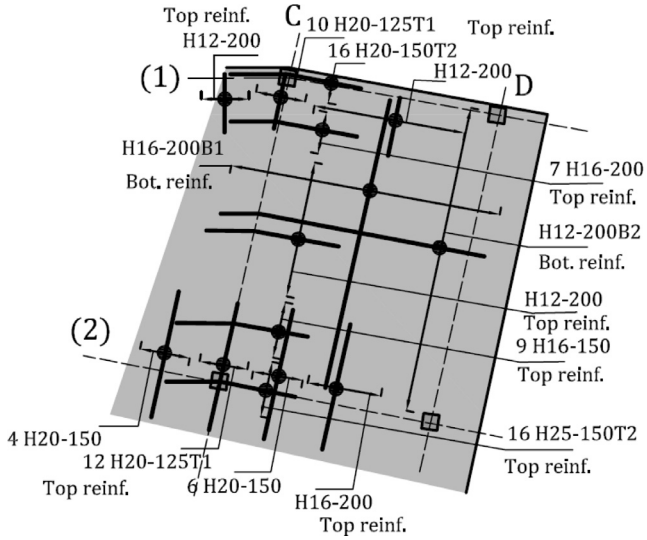

Fig. 3. Layout of the flexural reinforcement, adapted from CS [35].

Table 1
Considered load combinations.

Combination	Loads	Load value (kN/m^2)
Quasi-permanent	Dead + 0.3 Live	2.2
Frequent	Dead + 0.5 Live	3
Characteristic	Dead + Live	5
Overload	Dead + 1.5 Live	7

3.2. FE modelling of the structure

A finite element model is developed for the area of study in the flat slab building described in Section 3.1. FE software package LS-Dyna© [36] is applied in which the structural analyses are carried out in the time domain using an explicit algorithm to solve the motion equations considering material and geometric non-linearities. The flat slabs are modelled using Hughes-Liu shell elements [36], as shown in Fig. 4. The shell finite elements used are essentially composite layered elements with concrete and steel reinforcement layers similar to that used by [13]. The columns are modelled using a Belytschko-Schwer resultant beam elements [36] which are fully clamped at the foundation level and rigidly connected to each floor taking into account the size of the column. In the analysis, the columns are assumed to be non-critical; the assessment of flexural mechanisms is focused to the slabs. Edges 1 and 3 shown in Fig. 4(a) are free, whereas sides D and A represent points of contra-flexure. Fig. 4(b) shows the different reinforcement areas in the FE model of the slab and the FE mesh in the column and mid-span.

The constitutive material models adopted in the FE models take into account cracking and crushing of the concrete, as well as yielding, hardening and fracture of the reinforcement steel. The material models are based on the uniaxial behaviour with plastic-strain relationships. The concrete model adopted has a linear tension softening based on the fracture energy G_f and the Mander et al. [37] model for compression. The concrete model also takes into account the stiffness degradation due to cyclic loads (Young's modulus reduction).

The dead and live loads are applied in the FE model as masses uniformly distributed on the slab. In addition, concentrated masses are provided at the end edges (A and D in Fig. 4(a)). The gravity acceleration is introduced gradually over time using a ramp function ending at 0.8 s. This is followed by the column removal in a single time step ($\Delta t \approx 10^{-6}$ s).

3.3. Numerical results obtained in the column removal scenario

3.3.1. Predictions of slab rotation & dynamic amplification factors (DAFs)

Firstly, a quasi-static FE analysis was carried out for the column removal scenario with the frequent load combination. The quasi-static analysis was used to check the FE model in the elastic range before the column removal against the FE results obtained by [35]. Both FE models provide similar values for the column reactions and bending moments in the slab. Moreover, in the non-linear range, the quasi-static FE analysis provided consistent results with shear demand to rotation predictions from Model Code 2010 [30] using level of approximation II (LoA II) with $r_s = 0.22L_x$ as shown in Fig. 5(a); where r_s is the distance from the column axis to the zero radial moment and L_x is the span length. The reduction in slope after the column removal in the shear demand to rotation curve shown in Fig. 5(a) which is due to the residual spans, is captured adequately by the LoA II expression by considering the change in span L_x, i.e. $r_s = 0.22(2L_x)$.

Fig. 5(b) shows the slab rotation vs. shear demand obtained in the FE dynamic analyses for the frequent and characteristic load combinations; the comparison with the FE quasi-static curve illus-

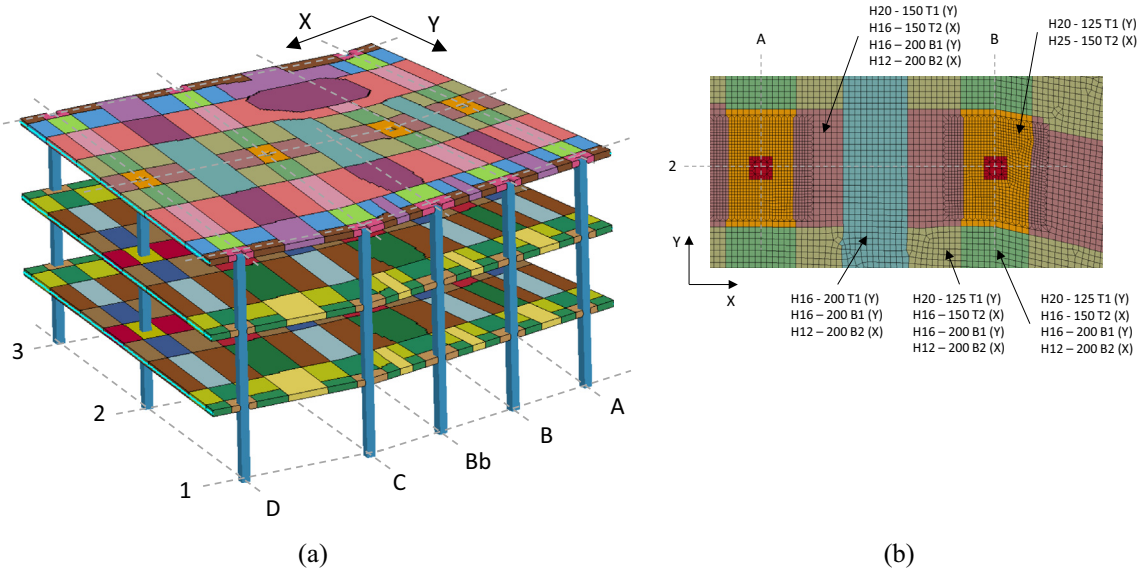

Fig. 4. Finite element model of the building considered in the case study: (a) perspective view of the 3D model and (b) local mesh and reinforced areas of the slab between two columns.

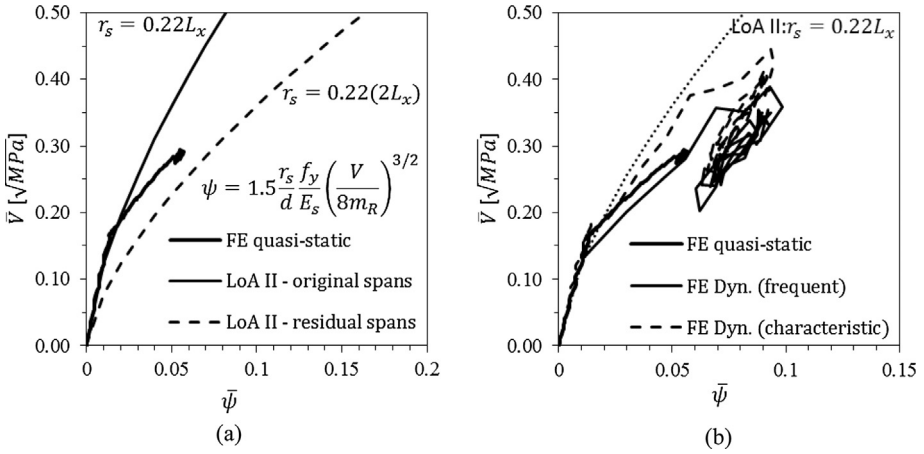

Fig. 5. Shear demand vs. slab rotation in column removal cases (a) quasi-static loading (effect of residual spans) and (b) dynamic FE analysis (influence of inertial effects).

trates the dynamic amplification of the slab rotation and shear demand. It is noteworthy in Fig. 5(b) that for high gravity loads (e.g. characteristic load), the inertial effects can result in a shear demand to rotation relationship which is not too different from the quasi-static one prior to the column removal with original spans (LoA II with $r_s = 0.22L_x$).

The dynamic amplification factor ($DAF = X_{dynamic}/X_{static}$) is used where X is the general structural response parameter. Fig. 6 shows the DAF obtained corresponding to three parameters: (a) the deflection at the removed column, (b) the slab rotation outside the column region and (c) the punching shear demand in the connection (DAF_{load}). Fig. 6 shows the results for the internal column B2 where the maximum DAF were 1.8 (slab rotation) and 1.36 (DAF_{load}). For the edge column C3, the maximum DAF were 1.64 (slab rotation) and 1.33 (DAF_{load}); all the results are summarized in Table 2. The DAF for the maximum deformation at mid-span was 1.9 as shown in Fig. 6(a).

The DAF_{load} obtained in this work was significantly lower than the theoretical value of 2.0 used in design which corresponds to the worst case scenario derived from a linear elastic system with instant removal and no damping. These differences are due to the influence in the inertial effects of material non-linear behaviour and damping. The values obtained for the DAF_{load} are consistent with those obtained experimentally in slab tests with column removal with similar levels of loading [19,23]. In Fig. 6(c), the residual DAF_{load} is 1.0 as expected with a total increase of shear demand of 70% between the quasi-static loading cases before and after the column removal. This increase in loading is justified due to the unequal spans in the slab and considerably larger contributable area of the removed column C2 compared to columns B2 and C3.

3.3.2. Punching shear assessment: EN 1992 vs. CSCT

This section shows the results from the assessment of the performance function and demand ratio in the column removal time history analysis following the approach in Fig. 1. The results are presented for the characteristic load combination (Table 1). Firstly, the variation of the coefficient of eccentricity is obtained for internal (B2) and edge (C3) columns. Fig. 7 shows the variation of coefficients β and k_e over time obtained according to Section 2.1; the horizontal dashed line represents the constant values recommended in EN 1992 and Model Code 2010 for internal and edge

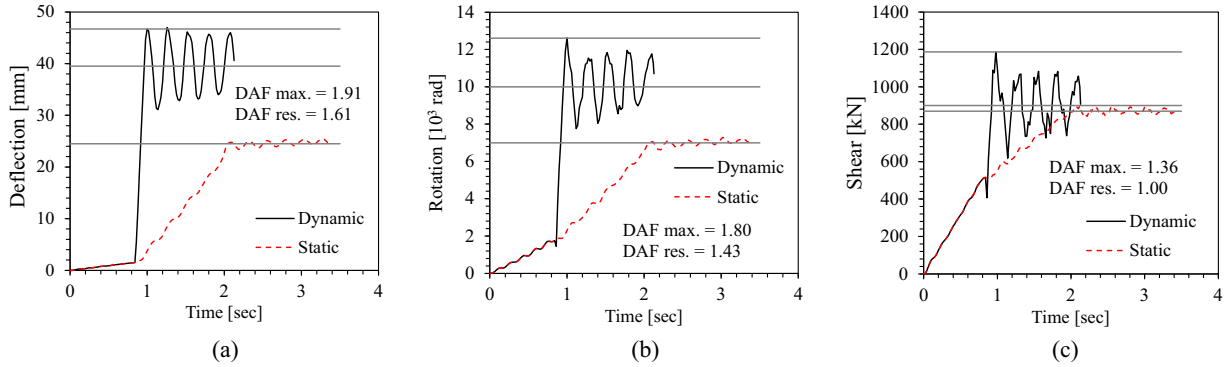

Fig. 6. Dynamic amplification factors obtained (frequent load combination): (a) ***DAF*** for deflection at the removed column (C2), (b) ***DAF*** for the maximum slab rotation outside internal column (B2), and (c) $\boldsymbol{DAF_{load}}$ for column (B2).

Table 2
DAFs obtained using the frequent slab load combination – internal and edge slab-column connections.

Deflection		Connection	Slab rotation		Punching shear demand	
Max.	Res.		Max.	Res.	Max.	Res.
1.91	1.61	Internal (B2)	1.80	1.43	1.36	1
		Edge (C3)	1.64	1.36	1.33	1

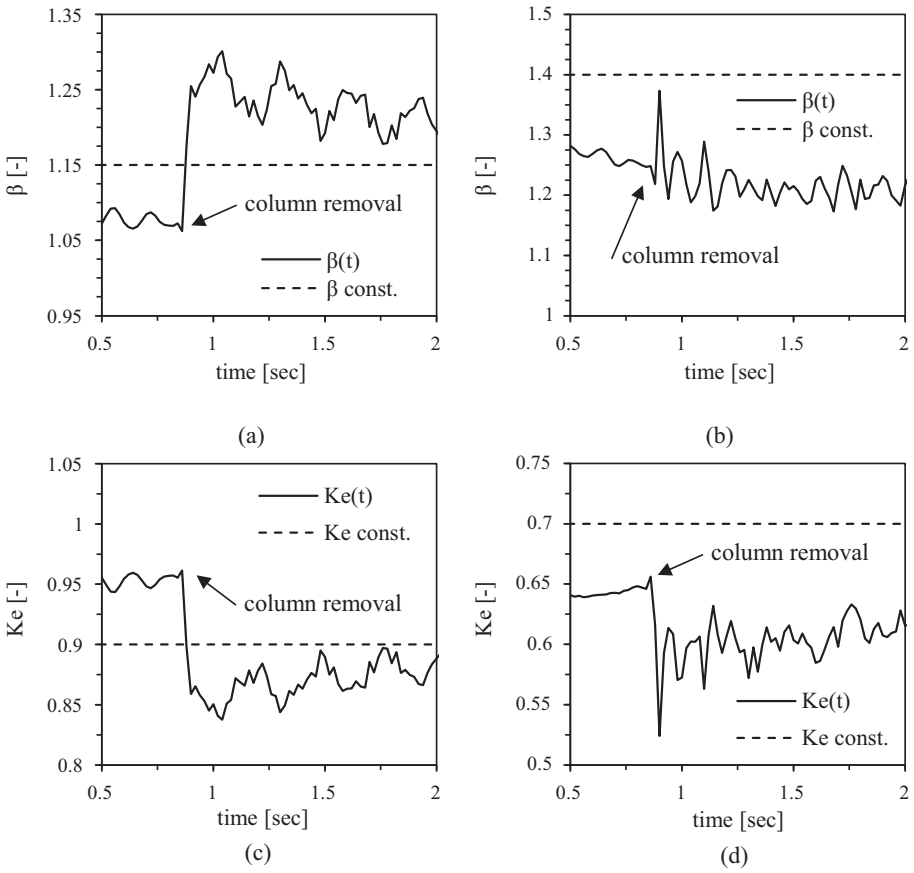

Fig. 7. Eccentricity coefficients (characteristic load): (a) and (b) EN 1992 approach for internal and edge connection respectively; (c) and (d) CSCT approach for internal and edge connection respectively.

columns with regular spans, which is only applicable prior to the column removal. The column removal results in a sudden increase of β (reduction of k_e), reaching a peak value at around 1 s. This is followed by fluctuations during the free vibration phase. The results for the internal column B2 show a larger variation in the coefficient of eccentricity compared to edge columns.

The eccentricities obtained in the analysis are considerable but they are within reasonable limits which are covered by existing

experimental testing of isolated punching shear tests (e/b_u between 0 and 2 according to database from Tassinari [38]). Therefore the formulae adopted in this work are applicable to the case investigated. For instance, internal column B2 develops eccentricities of 75 mm with $e/b_u = 0.05$ (prior to column removal, due to the geometry) and up to 240 mm with $e/b_u = 0.2$ (after column removal, due to residual spans and dynamic effects).

Fig. 8 shows the punching shear demand and capacity for the characteristic load combination during the time history according to EN 1992 and CSCT; solid lines represent the total values whereas dashed lines represent the concrete and reinforcement contributions separately. Points of intersection between V_D and $V_{C,cs}$ curves represent cases where punching shear is predicted to occur $Z(t) = 0$. Fig. 8 shows that according to both approaches, the internal column B2 would fail due to punching soon after the column removal (0.2 s). A similar conclusion is obtained for edge column C3.

The comparison between both approaches is carried out using the *DR* factor. Fig. 9 shows the *DR* obtained using both approaches for internal and edge columns B2 and C3 respectively. In all cases, *DR* reaches (or almost reaches) the value of 1.0 (i.e. punching failure is predicted to occur). In addition, just before the column removal both EN 1992 and CSCT approaches give very similar values of the *DR* for both internal and edge columns. For the internal column, the results given by both approaches after the column failure are also similar which suggests that for the levels of slab deformations achieved, the different assumptions made in each approach result in similar predictions. For edge columns, the CSCT gives slightly larger values of *DR*. The slight differences in the results for edge columns are somewhat expected since the behaviour of edge connections is less understood than for internal columns and therefore larger differences exist between capacity models.

The results shown in Fig. 9 indicate that punching is likely to occur after the column removal for the characteristic load combination. However, the maximum demand capacity ratio is very close to 1 in this case so the load and model uncertainties need to be taken into account to reach a more conclusive outcome. The maximum demand capacity ratio is different for each load combination considered, as shown in Fig. 10, where the maximum value of the *DR* is presented versus the total slab load. Fig. 10(a) and (b) shows that prior to the column removal punching will not occur ($DR < 1$) even for overload combination (DL + 1.5LL). Fig. 10(c) and (d) shows the predictions after the column removal where punching would only occur (internal/edge columns) according to both methods for loads greater than the frequent load combination. This suggests that the design of the structure is acceptable for accidental loading according to EN 1990 [6] in which only quasi-permanent and frequent load combinations are considered. In order to refine this assessment, a simplified reliability analysis is proposed in Section 4 considering the load uncertainty. Such analysis provides the reliability index and safety factor for different values of the probability of failure which could be used by the designer. For the following reliability analyses in this paper, only internal columns will be discussed.

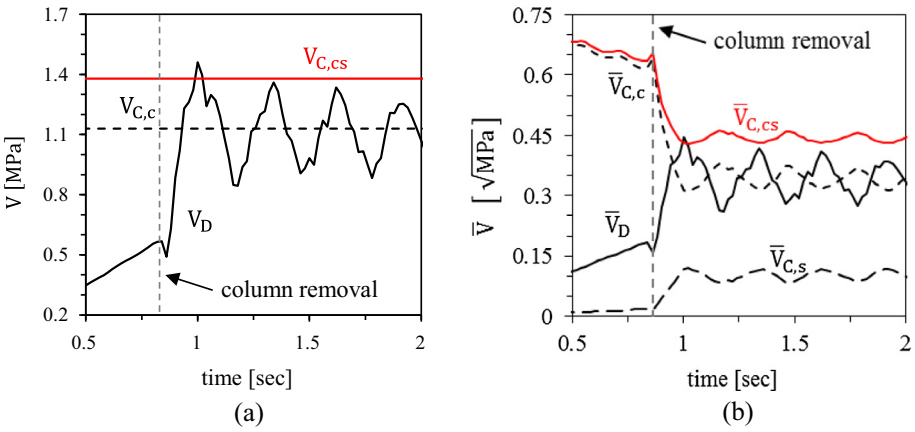

Fig. 8. Punching shear capacity and demand (characteristic load combination): (a) EN 1992 approach (constant capacity) and (b) CSCT approach (capacity varies with time).

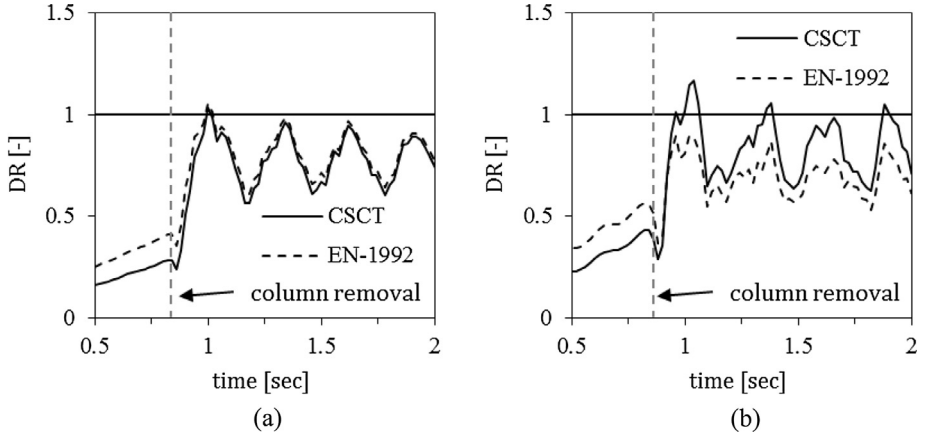

Fig. 9. Demand ratio in time history analysis (characteristic load combination): (a) internal column (B2) and (b) edge column (C3).

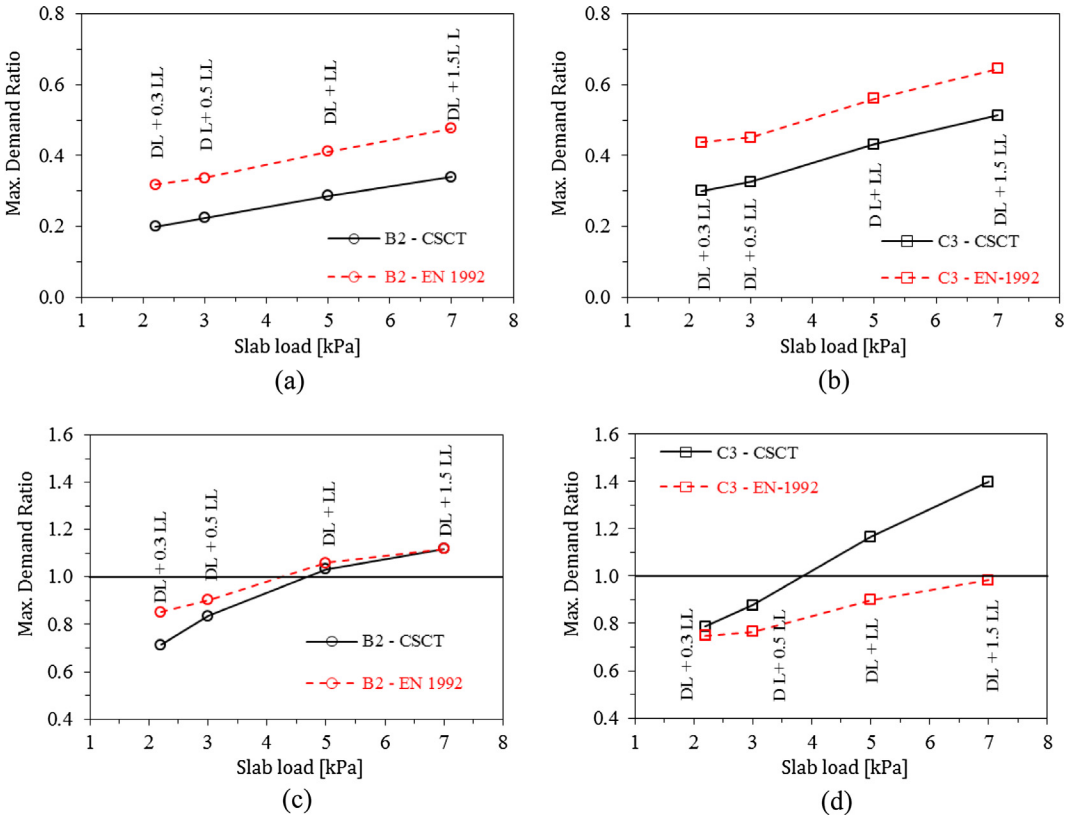

Fig. 10. Max demand ratio *DR* vs. slab load – (a) prior-column removal (internal column), (b) prior-column removal (edge column), (c) post-column removal (internal column) and (d) post-column removal (edge column).

4. Proposed simplified reliability analysis for punching shear

4.1. Fundamental assumptions

The assessment of the performance function of structures subjected to extreme loads can be problematic using a probabilistic framework unless some assumptions are made. Probabilistic performance-based design approaches have been proposed in the past by Val et al. [39], Ciampoli et al. [40] and Olmati et al. [41].

In case of severe structural damages simulated by the alternate load path method [7], the cause leading the column failure is neglected and the structural response of the building is assessed looking at the capacity of the structural elements to carry the overload due to the column removal. In the alternate load path analysis of buildings, the epistemic uncertainties related to the capacity model used are small compared to the uncertainties in the load conditions [41–43]. Therefore, the proposed simplified reliability analysis of structures subjected to exceptional loads considers mainly the variability of the gravity load on the slab; uncertainties in the spatial load distribution are not taken into account. Moreover, it is assumed that the occurrence of the load on the slab is not correlated with the occurrence of the structural damage. The obtained probability that the performance function is lower than zero is conditioned to the occurrence of the exceptional load. The alternate load path analysis is performed in a deterministic manner, as recommended by DoD [7]. In this context, Monte Carlo simulations involving structural analysis are not required and only a few structural analyses are needed. This advantage is particularly useful in the analysis of building structures since the numerical models needed have a high CPU demand. This is a novel probabilistic design procedure that is suitable with the alternate load path method that can be applied in the risk analysis of buildings at risk due to severe structural damages. The proposed simplified reliability method is a compromise in terms of complexity which can be useful for design purposes; more sophisticated probabilistic approaches (with added complexity) could be adopted in subsequent analysis to obtain a more refined answer.

4.2. Proposed methodology

The proposed methodology consists of three main steps: (a) to carry out a time history analysis of at least three load combinations (e.g. quasi-permanent, frequent and characteristic) to obtain the minimum value of Z for each case, (b) to estimate the probability density function PDF of the punching shear demand D_{PDF} by performing one Monte Carlo simulation and (c) to estimate the probability of $Z \leqslant 0$ by performing an additional Monte Carlo simulation. The two Monte Carlo simulations do not involve any additional structural analysis to those needed in step (a).

Fig. 11(a) summarizes all the intermediate steps required within the main steps (a, b, c). In step (a), the relationship between Z and D is assessed as well as the relationship between D and the slab load. In step (b), the slab load is assumed to follow a normal distribution and therefore D_{PDF} can be obtained from a Monte Carlo simulation. The response parameters (C, D, Z) can be linearized with respect to the slab load (see Section 4.4) and therefore it can be assumed that they also follow a normal distribution. In step (c), two alternative approaches are available to obtain the probability of failure $P[Z \leqslant 0]$, viz. directly from the PDF of Z according to Eq. (16) and from the reliability index β obtained from the PDF of C and D according to Eq. (17). Both approaches, which are summarized in Fig. 11(b), provide similar results.

$$P[Z \leqslant 0] = \int_{-\infty}^{0} p(z)dz = \Phi(-\beta) \tag{16}$$

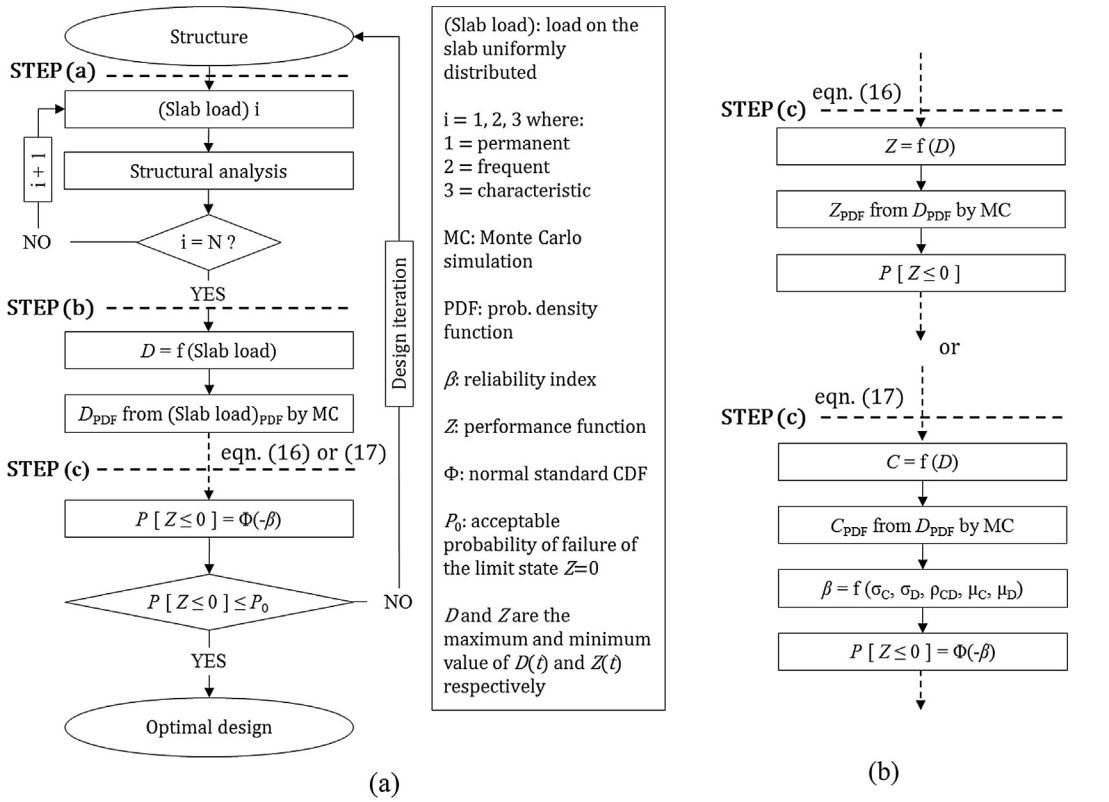

Fig. 11. Proposed methodology for reliability analysis of column-slab connections subjected to extreme loading: (a) flow chart of methodology and (b) alternative approaches to carry out step (c).

with $\beta = \mu_Z/\sigma_Z$ where μ_Z and σ_Z are the mean and standard deviation of Z respectively

$$P[Z = (C - D) \leqslant 0] = \Phi(-\beta) \tag{17}$$

with $\beta = \frac{\mu_C - \mu_D}{\sqrt{\sigma_C^2 + \sigma_D^2 - 2\rho_{CD}\sigma_C\sigma_D}}$ where μ_C and μ_D are the mean values of the punching shear capacity and demand respectively, σ_C and σ_D are standard deviation of the capacity and demand respectively and ρ_{CD} is the correlation coefficient between the capacity and demand, $|\rho_{CD}| = 1$ in this case. In case of using EN 1992 formulae, the standard deviation of C is zero since the capacity is independent of the load on the slab whereas in the CSCT, C is the distribution of the capacity corresponding to the values of the minimum Z obtained in step (a) and so $\sigma_C \neq 0$.

The effect of epistemic uncertainties in the capacity models can be investigated in a simplistic manner by using an arbitrary variability parameter $|\delta|$ which is introduced in the capacity function C in Eq. (17) as a percentage imperfection ranging from $-\delta$ to $+\delta$. The arbitrary epistemic uncertainty could be justified due to different simplifying assumptions in the capacity models, for example uncertainties in the capacity related to the effect of in-plane axial stresses in the slab (membrane action). In this work, 0 and 10% imperfection values are adopted for comparison in the assessment of $P[Z \leqslant 0]$; in cases where $|\delta| \neq 0$, Eq. (17) is adopted in which case $\rho_{CD} \neq 1$.

4.3. Acceptance criteria and definition of safety factor

In Fig. 11, P_0 is the acceptable probability of failure of the limit state $Z = 0$ conditioned to the structural damage. The recommended values of P_0 depend on the design situation and it is normally not specified in design codes. It is widely accepted in design for extreme events, that Low Probability High Consequence events have a different impact on the community than High Probability Low Consequence events HSE [11], FEMA [10], Barbato et al. [44]. In this work, a threshold value of P_0 between 0.01 and 0.1, with $\beta \approx 1.5$, is adopted. These threshold values were proposed by Ellingwood et al. [9] assuming that the accepted unconditional probability of failure for extreme loads is the same as the one accepted for the failure of structural elements subjected to live or dead loads.

In design, a safety factor λ given by Eq. (18) can be multiplied to the punching shear demand for the frequent load combination (expected value) to achieve an acceptable probability of failure P_0. This approach was proposed by Cornell et al. [45] for structures subjected to seismic load. Factor λ can also be used as an assessment check where $\mu_C/(\lambda\mu_D) > 1$ is considered to pass the check (valid design).

$$\lambda = e^{K_{P_0}\sigma_T} < \frac{\mu_C}{\mu_D} \tag{18}$$

where K_{P_0} is the standard normal variate to non-exceeding a probability of $(1 - P_0)$ which is obtained as $K_{P_0} = \Phi^{-1}(1 - P_0)$ and σ_T is the total standard deviation, which is obtained as $\sigma_T = \sqrt{\sigma_C^2 + \sigma_D^2 - 2\rho_{CD}\sigma_C\sigma_D}$; where μ_C and μ_D are the mean values of the punching shear capacity and demand respectively.

4.4. Example of application of proposed method to column removal scenario

The proposed method is applied to the column removal case described in Section 3. The results from step (a) corresponding to the time history analysis of the different load combinations are

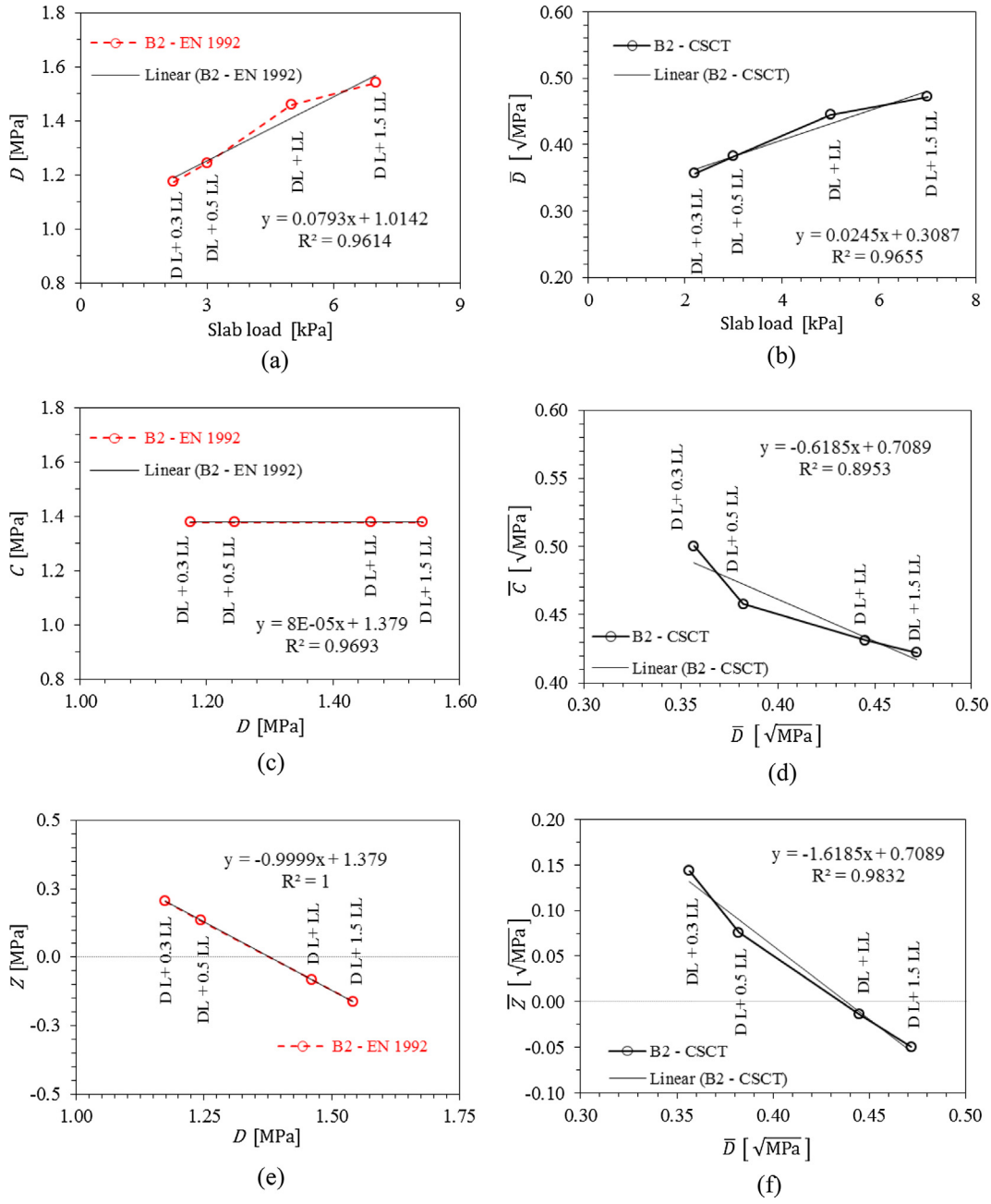

Fig. 12. Slab load, punching shear demand and capacity relationships – EN 1992 and CSCT procedures: (a) slab load vs. demand (EN 1992), (b) slab load vs. demand (CSCT), (c) demand vs. capacity (EN 1992), (d) demand vs. capacity (CSCT), (e) demand vs. performance function (EN 1992), and (f) demand vs. performance function (CSCT).

summarized in Fig. 12; the structural analysis is described in Section 3.3. Fig. 12 also shows the linear interpolated relationship obtained (with high value of R^2) between the slab load and the maximum value of $D(t)$ and the relationship with the minimum values of $C(t)$ and $Z(t)$. These relationships are needed in steps (b) and (c) of the proposed method (Fig. 11). The linearization is less accurate for the capacity using the CSCT which is expected; however this has a small influence on the results as the performance function is almost linear.

In step (b), the Monte Carlo simulation is carried out assuming a normal distribution of the slab load with mean and standard deviation equal to 3 kN/m^2 and 1.215 kN/m^2 respectively (refer to Table 1). Subsequently, the reliability index β and the probability of failure of the limit state $Z = 0$ are obtained in step (c). The results are summarized in Table 3, showing that EN 1992 and CSCT procedures give different values of the reliability index and therefore different probabilities of failure. However, the predictions are of the same order of magnitude. Both approaches provide values of

Table 3
Reliability index and probability of failure of the internal slab-column connection B2 according to the proposed method for the column removal scenario.

	EN 1992	CSCT
β with Eq. (16)	1.32	1.88
β with Eq. (17)	1.32	1.88
$P[Z \leqslant 0]$ with Eq. (16)	0.090	0.030
$P[Z \leqslant 0]$ with Eq. (17)	0.092	0.030
β with δ and Eq. (17)	1.01	1.66
$P[Z \leqslant 0]$ with δ and Eq. (17)	0.157	0.047

$P[Z \leqslant 0]$ within the acceptable threshold range of P_0 (0.01–0.1), although in the EN 1992, β is lower than 1.5.

Introducing the epistemic uncertainty in the capacity model δ results in a decrease in the reliability index (i.e. increase $P[Z \leqslant 0]$). Table 3 shows that considering an arbitrary value of 10% in the capacity model uncertainty, gives an increased value of $P[Z \leqslant 0]$ in the CSCT which is still below the threshold value. However, using the EN 1992 approach, $P[Z \leqslant 0]$ falls outside the threshold range and further analysis would be required considering the epistemic uncertainties in the capacity model.

Fig. 13 shows the safety factor λ obtained for different values of P_0 using the EN 1992 and CSCT approaches. The results shown in Fig. 13 are consistent with Table 3; λ is larger for the EN 1992 approach which reflects a larger dispersion in the capacity and demand distributions leading to lower values of the reliability index compared to the CSCT approach. Fig. 13(b) shows the values of $\mu_C/(\lambda\mu_D)$ used in the assessment check; it is shown that for the range of acceptable probabilities of failure 0.01–0.1, the design would only be valid for the CSCT.

5. Further applications of proposed approach to alternative damage scenarios

Alternative structural damage based scenarios can be considered to the column removal scenario. Two scenarios are investigated in this section, viz. falling slab scenario and a detonation close to the roof slab-column connection. The cause of these extreme events is not of relevance in this study; the results from the time history analysis are summarized for both cases as well as the results using the proposed reliability analysis.

5.1. Falling slab scenario

The study of progressive collapse of floor systems in multi-storey buildings subject to impact from debris or falling slab from above have been investigated in the past by researchers such as Vlassis et al. [2] for steel frame buildings. The shear demand in the slab-column connections is expected to be severe due to this event, considering the relative mass of the falling slab. For example, considering a 3.5 m storey height, the falling slab reaches a velocity of 8.3 m/s before the impact and therefore for every square metre of a 300 mm thick slab would transmit a kinetic energy of 25 kJ to the impacted slab. This energy estimation assumes a complete freefall which is an extreme case; in reality, a slower descent might take place.

In this work, an arbitrary portion of the second floor slab is dropped (complete freefall) into the first floor slab as shown in Figs. 14 and 15. The occurrence of punching of the slab-column connections B2 is assessed for this extreme event for comparison with the other damage scenarios; column C2 has a similar shear demand in this case. The arbitrary portion of the second floor slab is assumed to fail in three steps in order to induce some asymmetry in the impact. This assumption was adopted to obtain a more realistic and critical damage scenario with higher load eccentricities in the columns; assuming an idealised uniform vertical drop seems more suitable for design-based approaches. The variability

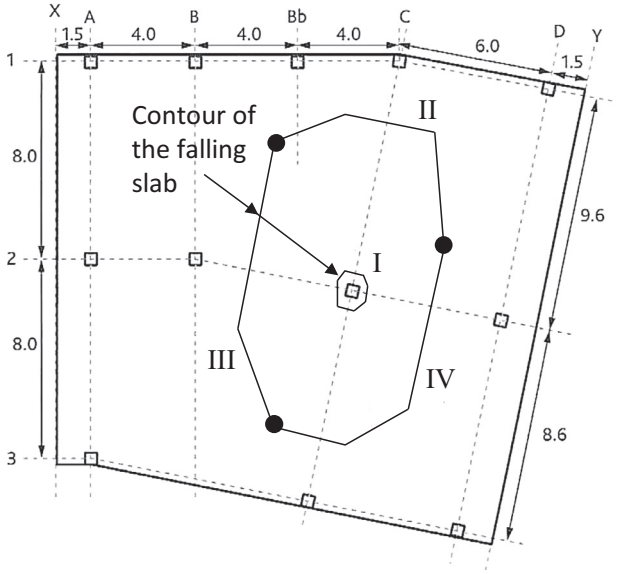

Fig. 14. Contour of falling slab (2nd floor), image adapted from CS [35].

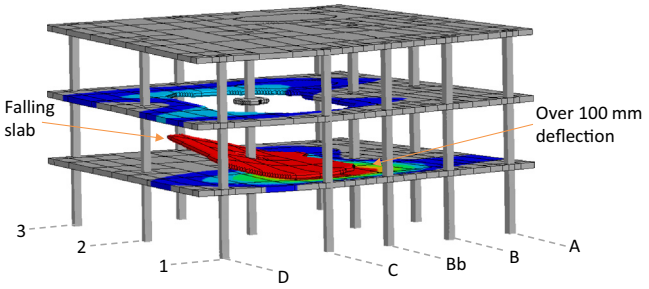

Fig. 15. FE model, portion of the second floor slab impacts the first floor slab (approximately 0.02 s after the first contact).

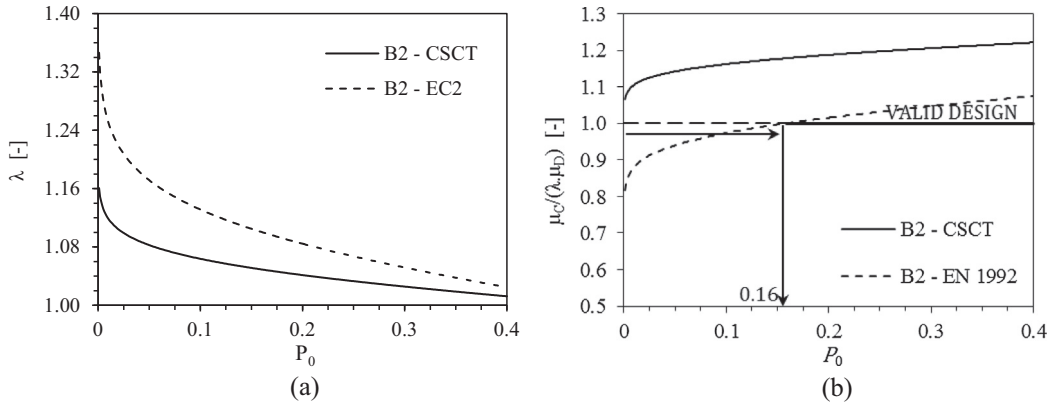

Fig. 13. Safety factor λ vs. P_0 obtained using the EN 1992 and CSCT in internal column B2: (a) factor λ to be multiplied by the deterministic demand for design purposes, (b) assessment check of structure.

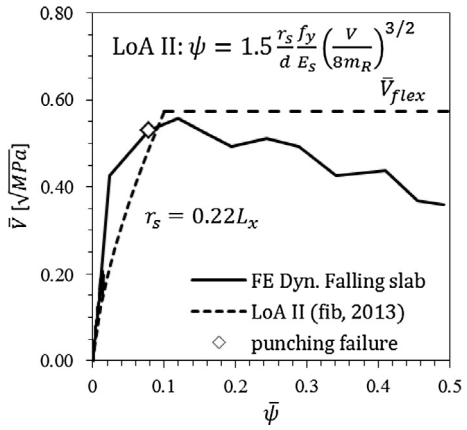

Fig. 16. Slab-column connection response for falling slab scenario (characteristic load combination).

of the size of the falling slab was not taken into account in this study. Fig. 14 shows the failing sequence of the falling slab; contour I fails initially around column C2 at the second floor which is followed by the failure of sections II, III and IV at every 0.15 s intervals between each. The falling slab impacts the floor below initially around the centre of the bay defined by gridlines B-C and 1–2 (Fig. 14).

Fig. 16 shows the development of the maximum slab rotation outside column B2 against the shear demand in the connection for the characteristic load combination; the parabolic formula LoA II in Model Code 2010 [30] provides reasonable predictions of the shear demand to rotation relationship before the impact at around $\overline{V} = 0.2\sqrt{\text{MPa}}$. The predictions from the dynamic FE model in Fig. 16 show a stiffer shear demand to rotation response after the impact due to inertial effects, which is consistent with impact behaviour of RC slabs described by Micallef et al. [32]. Punching is predicted to occur by the CSCT at a load near the flexural capacity of the slab ($\overline{V}_{flex}$) as shown in Fig. 16. The value of $\overline{V}_{flex}$ is estimated using the yield line method with a global mechanism in the impacted bay in the y direction considering the top reinforcement in the column and mid-span sections and bottom reinforcement at mid-span.

Fig. 17 shows the demand vs. capacity curves obtained in the time history analysis (characteristic load combination) for internal column B2; a sudden reduction of the punching capacity is obtained according to the CSCT whereas the capacity is constant according to EN 1992. The demand clearly exceeds the capacity soon after the slab impact according to both EN 1992 and CSCT approaches; the results obtained show that this is the case for the three main load combinations considered, even for the quasi-permanent load combination (Table 4). Similar results are obtained for internal column C2 which are not shown for conciseness.

The load variability is less relevant in this case due to the high demand ratio obtained as punching is predicted to occur in most cases of loading; *DR* reaches the value of 1 even in very unlikely load scenarios of around 1 kN/m^2 well below the quasi-permanent value. Therefore, in this case, the reliability analysis provides very high values of $P[Z \leqslant 0] \approx 0.98$ well above any acceptance criteria; the assessment check for $P_0 = 0.1$ would give values of $\mu_C/(\lambda\mu_D)$ equal to 0.67 well below 1.0. These results show that this damage scenario is critical and should be avoided in progressive collapses. This event can be mitigated to some extent by placing integrity reinforcement in the slab-column connection to hold the slab after punching failure [25].

5.2. Blast load scenario near column at the roof

A blast load scenario is considered in order to assess the susceptibility of slabs to punching around the connections in this case. This scenario consists of a detonation of 60 kg of TNT close to the roof slab-column connection B2 at 1 m stand-off distance above the slab; the exact position of the detonation is $\Delta X = 2.1$ m, $\Delta Y = 0$ m and $\Delta Z = 1$ m from column B2 (Fig. 2(b)). The stand-off

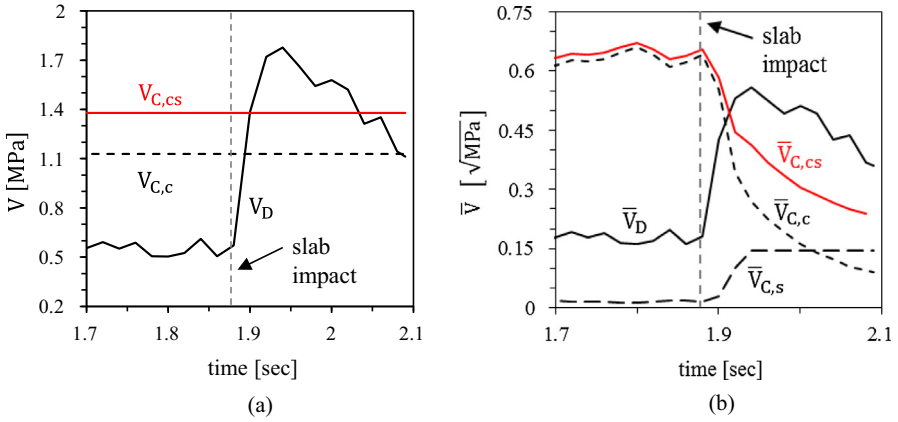

Fig. 17. Punching shear capacity and demand (characteristic load combination) for falling slab scenario (internal column B2): (a) EN 1992 approach and (b) CSCT approach.

Table 4
Maximum demand ratio for the falling slab and blast load scenarios.

Maximum *DR* Scenario and load combination	Falling slab scenario		Blast load scenario	
	EN 1992	CSCT	EN 1992	CSCT
Prior to the event (quasi-permanent load combination)	0.32	0.22	0.27	0.21
After the event (quasi-permanent load combination)	1.26	1.25	1.62	2.37
After the event (characteristic load combination)	1.28	1.75	1.72	2.75

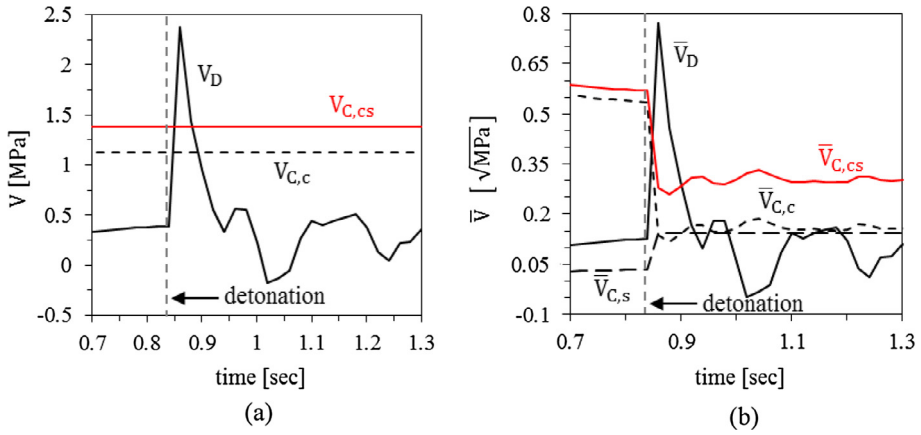

Fig. 18. Punching shear capacity and demand (characteristic load combination) for blast load scenario (internal roof connection B2): (a) EN 1992 approach and (b) CSCT approach.

distance is considered to be sufficient to avoid localized punching in the slab below the detonation point. The nature and magnitude of the close-in detonation considered is not relevant for the aim of this study.

The blast load is characterised as a pulse load with a sudden increase of overpressure followed by an approximately linear decay with time, until reaching a phase with negative pressures which is normally neglected for design purposes. The spatial distribution of the overpressures can be obtained numerically or using simplifying equations from the literature (e.g. Cormie et al. [46]). In this work, the blast demand was obtained using the numerical tool ConWep© in LS-Dyna© [36] which takes into account the time and space variations of the load, as well as the radial blast propagation (angle of incidence and increasing stand-off distance). ConWep can provide reasonable values of the reflected blast pressures for close-in detonations with scale distances of around 0.25 m/kg$^{1/3}$ as verified experimentally by Tyas et al. [47].

An additional dead and live load (distributed equivalent mass) were considered in the roof with an average value of 0.6 kN/m^2 and standard deviation of 0.25 kN/m^2. This imposed load represents normal design values for roofs not accessible except for normal maintenance and repair. The loads on the other floors are assumed to be equal to 5 kN/m^2.

Fig. 18 shows the results from the time history analysis for the characteristic load combination using EN 1992 and CSCT approaches. During the event, the punching shear demand increases suddenly after the detonation which is then followed by a reduction to its initial values before the blast. The slab has an impulsive behaviour in which the peak in the demand occurs well before the maximum deformations. The slab rotation increases significantly after the blast with a reduction of the capacity according to CSCT (Fig. 18). The maximum normalized slab rotation $\bar{\psi}$ is 0.16 at failure ($\overline{Z} = 0$) which is of similar magnitude to the rotations obtained in other damage scenarios.

For the blast considered, the demand induced is high, even larger than the falling slab case. The maximum demand ratio *DR* obtained for the given blast load is close to 2 using EN 1992 and CSCT (Table 4). *DR* is significantly higher than 1 even in the quasi-permanent load combination (i.e. the connection does not comply with the load combinations defined by EN 1990 for accidental loading). Similarly to the falling slab case, the variability of the load in the slab seems less critical in terms of assessing $P[Z \leqslant 0]$. In this case, step (c) in the reliability analysis (Fig. 11) seems unnecessary. It can be concluded that for the scale of the blast considered, emphasis should be made on the post-punching response of the slab to prevent progressive collapse, rather than preventing local failure.

6. Conclusions

The susceptibility to progressive collapse of RC flat slab buildings is highly dependent on the ability of slab-column connections to resist extreme loading. This paper investigates the structural behaviour of connections in flat slab buildings for three extreme events: column removal, slab falling from above and blast load. A simplified reliability approach is proposed to take into account uncertainty in the gravity load in the slab. The main conclusions are

1. The case study shows that prior to the extreme event, the demand ratio obtained using EN 1992 and CSCT approaches are similar. After the extreme event, the capacity reduces significantly with increasing slab rotation according to the CSCT, whereas the capacity remains constant using EN 1992 formulae. Despite this difference, both approaches provide similar values of the demand ratio after the column removal since the shear demand to rotation response in the dynamic case, with high gravity loads and residual spans, can be similar to that in a quasi-static case with original span layout.
2. In the quasi-static column removal scenario with a frequent gravity load combination, an increase of 70% in the shear demand was obtained in the adjacent column due to the irregular geometry investigated. In addition, a load dynamic amplification factor of 1.36 was obtained from the FE analysis. Both EN 1992 and CSCT confirmed that punching would only occur for gravity loads larger than the frequent combination value closer to the characteristic value, which can be considered acceptable according to EN 1990 design for accidental actions. This conclusion is consistent with the reliability studies.
3. In order to establish the probability of punching after column removal, the uncertainty in the gravity loads in the slab must be taken into account. The proposed reliability approach shows that the column removal scenario is not always critical. In fact, the probability of punching after column removal considering the uncertainty in the gravity load is within acceptable limits ($P[Z \leqslant 0] \leqslant 0.1$) according to both EN 1992 and CSCT. It is shown that neglecting epistemic uncertainties of the capacity models is a reasonable assumption in most cases; further work is needed for edge columns.
4. Falling slab from above, which has been observed in flat slab failures in the past, impose severe demand conditions to the slab-column connection. For the case investigated, the demand at the connection was near the flexural capacity for the characteristic load. The reliability analyses confirmed that the falling slab case is more critical than the column removal case; the

probability of punching due to this event is above threshold values. This supports the use of integrity reinforcement and other techniques to improve the post-punching behaviour of the connections to prevent progressive collapse.

5. The response of the slab in the blast load scenario is more impulsive compared to the column removal and falling slab scenarios, although the slab rotation outside the column at failure is of similar magnitude. Similarly to the falling slab case, the reliability approach showed that the connection is not able to withstand the increase of shear demand and emphasis should be placed on the post-punching response.
6. The falling slab and blast loading scenarios demonstrate that analyses considering the load causing the damage are also needed in practice since the consequences might not be fully covered using idealised column removal scenarios.
7. The variability in the gravity loads in the slab influences the inertial effects and demand capacity ratio of the slab-column connections after extreme events. The uncertainty in the load applied in the slab was found to have a less critical role in the falling slab and blast load cases considered due to the high shear demand compared to the column removal scenario. However, this might not be the case for other scenarios such as falling debris with smaller mass or blasts with lower charges than the ones adopted herein.

Acknowledgments

This work is part of a research project financially supported by the EPSRC Impact Acceleration Account held by the University of Surrey (grant ref: EP/K503939); linked with a previous project funded by the Engineering and Physical Sciences Research Council of the U.K. (grant ref: EP/K008153/1). Dr. Olmati is currently International Research Fellow (P-15786) of the Japan Society for the Promotion of Science (JSPS), Japan. Any opinions, findings, and conclusions or recommendations expressed in this article are those of the authors and do not necessarily reflect the views of the JSPS. The authors would also like to acknowledge project collaborators Prof. Aurelio Muttoni and Miguel Fernández Ruiz from EPFL (Switzerland) for their feedback and technical discussions on the topic.

References

[1] Regan PE. Behaviour of reinforced concrete flat slabs, Construction Industry Research and Information Association (CIRIA), Report 89; 1981. 89 pp.
[2] Vlassis AG, Izzudin BA, Nethercot DA. Progressive collapse of multi-storey buildings due to failed floor impact. Eng Struct 2009;31:1522–34.
[3] Krauthammer T. Modern protective structures. New York: CRC Press, Taylor & Francis Group; 2008.
[4] Starossek U, Haberland M. Disproportionate collapse: terminology and procedures. J Perform Constr Facil 2010;24(6):528. 528-519.
[5] Pidgeon N, O'Leary M. Man-made disasters: why technology and organizations (sometimes) fail. Saf Sci 2000;34:15–30.
[6] CEN Comité Européen de Normalisation. EN 1990: Eurocode – basis of structural design. Brussels, Belgium: CEN; 1990. p. 2002.
[7] DoD Department of Defense. Design of buildings to resist progressive collapse (UFC 4-023-03). Washington, DC: Unified Facilities Criteria; 2009.
[8] GSA General Services Administration. Progressive collapse analysis and design guidelines for new federal office buildings and major modernization projects. Washington, DC: Office of Chief Architect; 2000.
[9] Ellingwood BR, Smilowitz R, Dusenberry DO, Duthinh D, Carino NJ. Best practices for reducing the potential for progressive collapse in buildings. Washington, DC: National Institute of Standards and Technology; 2007.
[10] FEMA Federal Emergency Management Agency. Reference manual to mitigate potential terrorist attacks against building. Risk management series. Washington, DC; 2003.
[11] HSE Health and Safety Executive. Reducing risks, protecting people, HSE's decision-making process. HSE Books; 2001.
[12] Mohamed OA. Progressive collapse of structures: annotated bibliography and comparison of codes and standards. J Perform Constr Facil 2006;20(4):418–25.
[13] Szyniszewski S, Krauthammer T. Energy flow in progressive collapse of steel framed buildings. Eng Struct 2012;42:142–53.
[14] Abruzzo J, Matta A, Panariello G. Study of mitigation strategies for progressive collapse of a reinforced concrete commercial building. J Perform Constr Facil 2006;20(4):384–90.
[15] Kokot S, Anthoine A, Negro P, Solomos G. Static and dynamic analysis of a reinforced concrete flat slab frame building for progressive collapse. Eng Struct 2012;40:205–17.
[16] Helmy H, Salem H, Mourad S. Computer-aided assessment of progressive collapse of reinforced concrete structures according to GSA code. J Perform Constr Facil 2013;27(5):529–39.
[17] Mitchell D, Cook WD. Preventing progressive collapse of slab structures. ASCE J Struct Eng 1984;110:1513–32.
[18] Utagawa N, Kondo I, Yoshida N, Itho N, Yoshida N. Simulation of demolition of reinforced concrete buildings by controlled explosion. Comput-Aided Civ Infrastruct Eng 1992;7(2):151–9.
[19] Qian K, Bing L. Experimental study of drop-panel effects on response of reinforced concrete flat slabs after loss of corner column. ACI Struct J 2013;110 (2):319–30.
[20] Liu J, Tian Y, Orton SL, Said AM. Resistance of flat-plate buildings against progressive collapse. I: Modelling of slab-column connections. J Struct Eng 2015;141(12).
[21] Liu J, Tian Y, Orton SL, Said AM. Resistance of flat-plate buildings against progressive collapse. II: system response. J Struct Eng 2015;141(12).
[22] Dat PX, Hai TK. Membrane actions of RC slabs in mitigating progressive collapse of building structures. Eng Struct 2013;55:107–15.
[23] Russell JM, Owen JS, Hajirasouliha I. Experimental investigation on the dynamic response of RC flat slabs after a sudden column loss. Eng Struct 2015;99:28–41.
[24] Keyvani L, Sasani M, Mirzaei Y. Compressive membrane action in progressive collapse resistance of RC plates. Eng Struct 2014;59:554–64.
[25] Melo GS, Regan PE. Post-punching resistance of connections between flat slabs and interior columns. Mag Concr Res 1998;50(4):319–27.
[26] Fernández Ruiz M, Mirzaei Y, Muttoni A. Post-punching behavior of flat slabs. ACI Struct J 2013;110(5):801–12.
[27] CEN Comité Européen de Normalisation. EN 1992-1-1: design of concrete structures – Part 1-1: general rules and rules for buildings. Brussels, Belgium: CEN; 2004.
[28] Muttoni A. Punching shear strength of reinforced concrete slabs without transverse reinforcement. ACI Struct J 2008;105(4):440–50.
[29] Fernández Ruiz M, Muttoni A. Applications of the critical shear crack theory to punching of R/C slabs with transverse reinforcement. ACI Struct J 2009;106 (4):485–94.
[30] fib Fédération internationale du béton. fib Model code for concrete structures 2010. Berlin: Ernst & Sohn; 2013. 434 p.
[31] Sagaseta J, Muttoni A, Fernández Ruiz M, Tassinari L. Non-axis-symmetrical punching shear around internal columns of RC slabs without transverse reinforcement. Mag Concr Res 2011;63(6):441–57.
[32] Micallef K, Sagaseta J, Fernández Ruiz M, Muttoni A. Assessing punching shear failure in reinforced concrete flat slabs subjected to localised impact loading. Int J Impact Eng 2014;71:17–33.
[33] Schultz MT, Gouldby BP, Simm JD, Wibowo JL. Beyond the factor of safety: developing fragility curves to characterize system reliability ERDC SR-10-1, US. The United States Army Corps of Engineers: Engineer Research and Development Center; 2010.
[34] Olmati P, Petrini F, Bontempi F. Numerical analyses for the structural assessment of steel buildings under explosions. Struct Eng Mech 2013;45 (6):803–19.
[35] CS Concrete Society. Guide to the design and construction of reinforced concrete flat slabs. Technical report 2007; no 64; 2007. 101 pp.
[36] LSTC Lawrence Software Technology Corporation. LS-DYNA theory manual. Livermore, California: Livermore Software Technology Corporation; 2012.
[37] Mander JB, Priestley MJN, Park R. Theoretical stress-strain model for confined concrete. J Struct Eng 1998;114:1804–26.
[38] Tassinari L. Poinçonnement non symétrique des dalles en béton armé. PhD thesis. École Polytechnique Fédérale de Lausanne, no 5030; 2011. 163 pp [in French].
[39] Val DV, Stewart MG, Melchers RE. Life-cycle performance of RC bridges: probabilistic approach. Comput-Aided Civ Infrastruct Eng 2000;15(1): 14–25.
[40] Ciampoli M, Petrini F, Augusti G. Performance-based wind engineering: towards a general procedure. Struct Saf 2011;33(6):367–78.
[41] Olmati P, Petrini F, Gkoumas K. Fragility analysis for the performance-based design of cladding wall panels subjected to blast load. Eng Struct 2014;78:112–20.
[42] Fragiadakis M, Vamvatsikos D, Karlaftis MG, Lagaros ND, Papadrakakis M. Seismic assessment of structures and lifelines. J Sound Vib 2015;334: 29–56.
[43] Olmati P, Trasborg P, Naito CJ, Bontempi F. Blast resistant design of precast reinforced concrete walls for strategic infrastructures under uncertainty. Int J Crit Infrastruct 2015;11(3):197–212.
[44] Barbato M, Petrini F, Unnikrishnan VU, Ciampoli M. Performance-based hurricane engineering (PBHE) framework. Struct Saf 2013;45:24–35.

[45] Cornell CA, Jalayer F, Hamburger RO, Foutch DA. Probabilistic basis for 2000 sac federal emergency management agency steel moment frame guidelines. J Struct Eng 2008;128(4):526–33.
[46] Cormie D, Mays G, Smith P. Blast effects on buildings, 2nd ed.. London: ICE Publishing; 2012.
[47] Tyas A, Reay J, Warren JA, Rigby SE, Clarke SD, Fay SD, Pope DJ. Experimental studies of blast wave development and target loading from near-field spherical PETN explosive charges. In: 16th international symposium on 3 the interaction of the effects of munitions with structures (ISIEMS), Florida, 2015.